

Saturation corrections to dilute-dense particle production and azimuthal correlations in the Color Glass Condensate

S. Schlichting¹ and V. Skokov^{2,3}

¹*Fakultät für Physik, Universität Bielefeld, D-33615 Bielefeld, Germany*

²*Department of Physics, North Carolina State University, Raleigh, NC 27695*

³*RIKEN-BNL Research Center, Brookhaven National Laboratory, Upton, NY 11973*

(Dated: October 29, 2019)

Abstract

We perform a numerical study of higher order saturation corrections to the dilute-dense approximation for multi-particle production in high-energy hadronic collisions in the framework of the Color Glass Condensate. We compare semi-analytical results obtained by performing a leading order expansion in the dilute field of the projectile with numerical simulations of the full Classical Yang-Mills dynamics for a number of phenomenologically relevant observables. By varying the saturation momentum of the target and the projectile, we establish the regime of validity of the dilute-dense approximation and assess the magnitude and basic features of higher order saturation corrections. In particular, we find that dilute-dense approximation faithfully reproduces dense-dense results if restricted to the range of its validity.

I. INTRODUCTION

Describing multiple production of semi-hard particles in high-energy hadronic collisions is a challenging task, which in general is not well understood theoretically. At asymptotically high energies, the Color Glass Condensate effective theory (see e.g. [1]) provides a viable approach to describe multi-particle production, including correlations between the produced particles. In its simplest form the colliding hadrons are approximated by two sheets of Classical Yang-Mills field $A \sim \mathcal{O}(g^{-1})$ with quantum corrections suppressed by extra powers of strong coupling constant g . Particle production can be described by the classical gluon fields after the collision in the forward light cone. Within this framework, an analytical approach is possible when one of the objects can be considered as “dilute” $A \sim \mathcal{O}(g^0)$. This allows one to perform the expansion in the measure of the diluteness, usually quantified by the projectile saturation momentum $Q_s^{(P)}$. Conversely, if both colliding objects are “dense” $A \sim \mathcal{O}(g^{-1})$, a full set of classical Yang-Mills equations has to be solved. The authors are not aware if even a distant possibility of having an analytical result exists in this case.

A. Particle production in classical approximation.

In order to review the current theoretical status of particle production in the saturation/CGC formalism, let us first consider single inclusive particle production. Schematically, the single inclusive particle gluon spectrum can be expressed as (see Ref. [2] for more details):

$$\frac{dN}{d^2kdy} = \frac{1}{\alpha_s} f \left(\frac{Q_s^{(P)2}}{k^2}, \frac{Q_s^{(A)2}}{k^2} \right), \quad (1)$$

where $Q_s^{(P)}$ and $Q_s^{(A)}$ are the saturation momenta for the projectile and target and α_s is the strong coupling constant. In the pioneering works of [3–6], the function f was studied numerically by solving Classical Yang-Mills (CYM) equations and projecting the classical field onto transversely polarized gluon states (see e.g. Ref. [7]); we will perform similar calculations in this work. So far the only known situation which is analytically tractable, is an expansion of f in either one of its arguments $\frac{Q_s^{(P)2}}{k^2}$ and/or $\frac{Q_s^{(A)2}}{k^2}$. In the *dilute-dense* approximation designed for asymmetric collision systems (e.g. p-A), one assumes that for a given transverse momentum k of interest the projectile is a dilute object, $Q_s^{(P)2}/k^2 \lesssim 1$.

This allows for a systematic expansion of the production cross section in this parameter

$$\frac{dN}{d^2kdy} = \frac{1}{\alpha_s} \left[\frac{Q_s^{(P)^2}}{k^2} f_1 \left(\frac{Q_s^{(A)^2}}{k^2} \right) + \left(\frac{Q_s^{(P)^2}}{k^2} \right)^2 f_2 \left(\frac{Q_s^{(A)^2}}{k^2} \right) + \dots \right]. \quad (2)$$

Specifically, the function f_1 is known analytically for about two decades (see Refs. [8–10]); at this (leading) order the number of produced gluons for given projectile and target configurations is given by

$$\left. \frac{dN}{d^2kdy} \right|_{\rho_p, \rho_t} = \frac{2g^2}{(2\pi)^3} \int \frac{d^2q}{(2\pi)^2} \frac{d^2q'}{(2\pi)^2} \Gamma(\vec{k}_\perp, \vec{q}_\perp, \vec{q}'_\perp) \rho_p^a(-\vec{q}'_\perp) \left[U^\dagger(\vec{k}_\perp - \vec{q}'_\perp) U(\vec{k}_\perp - \vec{q}_\perp) \right]_{ab} \rho_p^b(\vec{q}_\perp), \quad (3)$$

for a fixed configuration of color charges ρ_p, ρ_t in the dilute projectile (p) and dense target (t). Here $\Gamma(\vec{k}_\perp, \vec{q}_\perp, \vec{q}'_\perp)$ is the square of Lipatov vertex, see Ref. [11] or the main body of the paper for details. Although, equation (3) is only quadratic in ρ_p , it contains all orders of ρ_t , which are re-summed in the adjoint Wilson line U , representing the eikonal scattering matrix for scattering of a single gluon on the target.

While Eq. (3) provides the leading order in the dilute-dense expansion of Eq. (2), the function f_2 , is also termed as the *first saturation correction* in the projectile, since it comes along with two powers of $Q_s^{(P)^2}/k_\perp^2$, corresponding to interactions with two valence sources in the projectile. Efforts to calculate f_2 analytically are detailed in Ref. [12] and more recently in Ref. [13]. However, at present, f_2 is known only partially.

In summary, higher order corrections, functions f_i for $i \geq 2$, to the strict dilute-dense approximation, f_1 , are presently not known analytically. Even if analytical forms of f_i were known, they may still involve rather complicated momentum integrals of Wilson lines of the target field, see e.g. Eq. (3). Hence, it is practically inevitable to use numerical methods (typically involving lattice discretization) and we will therefore refer to this as a semi-analytical approach.

Nevertheless, in contrast to CYM simulations, semi-analytical calculations based on f_i neither require a numerical solution of the gauge field evolution in the forward light-cone nor a numerical implementation of LSZ reduction. Besides, one additional advantage of this semi-analytic dilute-dense approach is that it facilitates the inclusion of small- x evolution, running coupling corrections, as well as higher order α_s corrections, in contrast to fully numerical CYM simulations. It is also superior in terms of simulation time and thus allows for an easier access to the continuum limit. However, the obvious drawback of this approach

is that it may miss a potentially large contribution from the higher order expansion coefficients. Hence, the goal of this paper is to perform a systematic numerical study of the saturation corrections and to compare them with leading order dilute-dense approximation.

So far we have focused on single inclusive particle production; however an analogous discussion also applies to the multi-particle production. Specifically, the double inclusive two-gluon spectrum can be written in the following form,

$$\frac{dN}{d^2k_1 dy_1 d^2k_2 dy_2} = \frac{1}{\alpha_s^2} h \left(\frac{Q_s^{(P)2}}{k^2}, \frac{Q_s^{(A)2}}{k^2} \right) \quad (4)$$

with a new unknown function h . Here k_1 and k_2 are the gluons' transverse momenta and we assumed that $|k_1| = |k_2| = k$ to simplify notation. By considering a dilute projectile, we can again expand in $Q_s^{(P)2}/k_\perp^2$, which results in

$$\frac{dN}{d^2k_1 dy_1 d^2k_2 dy_2} = \frac{1}{\alpha_s^2} \left[\left(\frac{Q_s^{(P)2}}{k^2} \right)^2 h_1 \left(\frac{Q_s^{(A)2}}{k^2} \right) + \left(\frac{Q_s^{(P)2}}{k^2} \right)^3 h_2 \left(\frac{Q_s^{(A)2}}{k^2} \right) + \dots \right], \quad (5)$$

where the function h_1 can be found from the results of Refs. [14–16] and is also written in convenient form for numerical simulations in Refs. [17]. Compared to f_1 in Eq. (3), which features two target Wilson lines (dipole), the function h_1 involves four Wilson lines (quadrupole). It is well known [14, 15], that this part of the two-gluon production cross section is invariant under the reflection of either momenta k_1 or k_2 and thus generates only even harmonics of azimuthal anisotropy. More recently, in Refs. [2, 18], it was shown that this accidental symmetry with respect to the reflection of one of the momenta is lifted by the first saturation contribution, h_2 , to double inclusive production. In particular, the part of h_2 responsible for the odd harmonics was derived analytically [2, 18]. Nevertheless, the full result for h_2 (including also the first saturation corrections to the even part) is currently unknown and would require determination of f_2 .

In the current study, we will use semi-analytical results for f_1 , h_1 and the odd part of h_2 in order to compute the observables dN/dy , v_2 , v_4 and v_3 which are of particular relevance to phenomenological CGC studies [7, 11, 17, 19–22]. By explicitly comparing the results for these observables with the corresponding ones obtained in full dense-dense calculations of Eqs. (1) and (4) based on CYM simulations, we will assess the quality of the dilute-dense approximation and the impact of higher order saturation corrections.

II. DILUTE-DENSE VS. DENSE-DENSE – EXPLICIT RESULTS AND COMPARISON

A. General Setup

We consider the color charge distribution in the dilute projectile as

$$\langle \rho_a^{(p)}(\vec{x}_\perp) \rho_b^{(p)}(\vec{x}'_\perp) \rangle = \left(\frac{g^2 \mu}{Q_s} \right)^2 Q_s^{(P)2} \left(\frac{\vec{x}_\perp + \vec{x}'_\perp}{2} \right) \delta_{ab} \delta^{(2)}(\vec{x}_\perp - \vec{x}'_\perp), \quad (6)$$

where the local saturation scale $Q_s^{(P)2}(\vec{x}_\perp)$ is determined by

$$Q_s^{(P)2}(\vec{x}_\perp) = 2\pi R_p^2 T(\vec{x}_\perp) (Q_{s,0}^{(p)})^2 = (Q_{s,0}^{(p)})^2 \exp\left(-\frac{\vec{x}_\perp^2}{2R_p^2}\right) \quad (7)$$

such that the dilute projectile can be thought of as a minimal saturation model for the proton. We note that in order to scrutinize the particle production mechanism we restrict ourselves to such a minimal model, and have not included additional ingredients, such as e.g. sub-nucleonic constituents [23, 24] or saturation scale $(Q_{s,0}^{(p)})^2$ fluctuations [25] commonly invoked in phenomenological CGC calculations. Similarly, we consider a spatially homogeneous color charge distribution of the dense target, i.e.

$$\langle \rho_a^{(t)}(\vec{x}_\perp) \rho_b^{(t)}(\vec{x}'_\perp) \rangle = \left(\frac{g^2 \mu}{Q_s} \right)^2 (Q_{s,0}^{(A)})^2 \delta_{ab} \delta^{(2)}(\vec{x}_\perp - \vec{x}'_\perp) \quad (8)$$

which likewise, can be thought of as a simplistic saturation model of a very large nucleus. We note that the parameter $(Q_{s,0}^{(A)})^2$ characterizes the saturation scale everywhere in the large nucleus, whereas $(Q_{s,0}^{(p)})^2$ gives the saturation scale of the proton in the center, such that on average the saturation momentum in the proton is somewhat smaller, e.g. $\langle Q_s^2(\vec{x}_\perp) \rangle|_{|\vec{x}_\perp| < R_p} \approx 0.79 (Q_{s,0}^{(p)})^2$.

Since the common prefactor $\left(\frac{g^2 \mu}{Q_s}\right)$ can always be absorbed into a redefinition of the saturation momenta $Q_{s,0}^{(p/A)}$, we will always fix its value to $\left(\frac{g^2 \mu}{Q_s}\right) = 1.42857$ – a typical value employed in phenomenological studies in IP-Glasma [26, 27]. Besides the projectile size R_p and the saturation momenta $Q_{s,0}^{(p/A)}$ of the projectile and target, our model then only has one additional parameter m which regulates the infrared behavior of the color charge distributions. We again follow previous works [26, 27], and adopt the common procedure to replace

$$\rho_a(\vec{p}_\perp) \rightarrow \frac{\vec{p}_\perp^2}{\vec{p}_\perp^2 + m^2} \rho_a(\vec{p}_\perp) \quad (9)$$

in our numerical calculations, where evidently $Q_{s,0}^{2(p/A)} \gg m^2$ should hold to minimize the sensitivity to the infrared regulator. If not stated otherwise, we will fix $R_p = 2 \text{ GeV}^{-1}$ and $m = 0.5 \text{ GeV}$ in the following and compare results for particle production in dilute-dense and dense-dense calculations as a function of the saturation scales $Q_{s,0}^{(p)}$ and $Q_{s,0}^{(A)}$ of the projectile and target.¹ Details of the individual calculations proceed as described as outlined below, and are described in detail in Ref. [22] for dilute-dense and Ref. [7] for dense-dense calculations.

B. Dilute-dense approximation

We briefly review the **dilute-dense** expressions derived previously in Refs. [2, 8–10, 14, 15, 18]). Starting from a statistical sampling of the color charge distribution ρ_p and ρ_t of the projectile and target according to Eqns. (6,8), the leading contribution to the configuration-by-configuration spectrum is then given by Eq. (3) with

$$\Gamma(\vec{k}_\perp, \vec{q}_\perp, \vec{q}'_\perp) = \left(\frac{\vec{k}_\perp}{k^2} - \frac{\vec{q}_\perp}{q^2} \right) \cdot \left(\frac{\vec{k}_\perp}{k^2} - \frac{\vec{q}'_\perp}{q'^2} \right). \quad (10)$$

However, as alluded to in the Sec. I, the form (3) is, not particularly useful for numerical calculations, as it involves two two-dimensional, not obviously factorizable integrals. Instead one can recast (3) in fully equivalent form

$$\frac{dN^{\text{even}}(\vec{k}_\perp)}{d^2k dy} [\rho_p, \rho_t] = \frac{2}{(2\pi)^3} \frac{\delta_{ij}\delta_{lm} + \epsilon_{ij}\epsilon_{lm}}{k^2} \Omega_{ij}^a(\vec{k}_\perp) \left[\Omega_{lm}^a(\vec{k}_\perp) \right]^* \quad (11)$$

with $\Omega(\vec{k}_\perp)$ defined as the Fourier transform of

$$\Omega_{ij}^a(\vec{x}_\perp) = g \left[\frac{\partial_i}{\partial^2} \rho_p^b(\vec{x}_\perp) \right] \partial_j U_{ab}(\vec{x}_\perp), \quad (12)$$

and $\epsilon_{ij}(\delta_{ij})$ denotes the Levi-Civita symbol (Kronecker delta). The adjoint Wilson line U_{ab} is a functional of the target charge density:

$$U(\vec{x}_\perp) = \mathcal{P} \exp \left(ig^2 \int dx^+ \frac{1}{\partial^2} \rho_t^a(x^+, \vec{x}_\perp) T_a \right). \quad (13)$$

The expression in Eq. (11) explicitly demonstrates that numerical evaluation of the even component boils down to a straightforward computation of two combination $\epsilon_{ij}\Omega_i^a j(\vec{x}_\perp)$ and

¹ Stated differently we set the dimensionless parameter $mR_p = 1$ and use $R_p = 2 \text{ GeV}^{-1}$ to set the scale in our calculation.

$\delta_{ij}\Omega_{ij}^a(\vec{x}_\perp)$ complemented by the fast Fourier transformation. As discussed in Introduction, the odd component of the particle production cross section is given by higher order corrections to the strict dilute-dense limit. The leading contribution is

$$\frac{dN^{\text{odd}}(\vec{k}_\perp)}{d^2kdy}[\rho_p, \rho_t] = \frac{2}{(2\pi)^3} \text{Im} \left\{ \frac{g}{\vec{k}_\perp^2} \int \frac{d^2l}{(2\pi)^2} \frac{\text{Sign}(\vec{k}_\perp \times \vec{l}_\perp)}{l^2 |\vec{k}_\perp - \vec{l}_\perp|^2} f^{abc} \Omega_{ij}^a(\vec{l}_\perp) \Omega_{mn}^b(\vec{k}_\perp - \vec{l}_\perp) \left[\Omega_{rp}^c(\vec{k}_\perp) \right]^* \right. \\ \left. \times \left[\left(\vec{k}_\perp^2 \epsilon^{ij} \epsilon^{mn} - \vec{l}_\perp \cdot (\vec{k}_\perp - \vec{l}_\perp) (\epsilon^{ij} \epsilon^{mn} + \delta^{ij} \delta^{mn}) \right) \epsilon^{rp} + 2\vec{k}_\perp \cdot (\vec{k}_\perp - \vec{l}_\perp) \epsilon^{ij} \delta^{mn} \delta^{rp} \right] \right\}. \quad (14)$$

We emphasize that in a Gaussian model for the projectile the above expression does *not* contribute to single inclusive cross section due to $\left\langle \frac{dN^{\text{odd}}(\vec{k}_\perp)}{d^2kdy}[\rho_p, \rho_t] \right\rangle = 0$, but does contribute to the double inclusive production.

Based on the configuration-by-configuration spectrum, the single and double inclusive gluon production cross section are then given in terms of the statistical averages of the respective operators

$$\frac{dN(\vec{k}_\perp)}{d^2kdy} = \left\langle \frac{dN(\vec{k}_\perp)}{d^2kdy}[\rho_p, \rho_t] \right\rangle, \quad (15)$$

$$\frac{d^2N(\vec{k}_{1\perp}, \vec{k}_{2\perp})}{d^2k_1 dy_1 d^2k_2 dy_2} = \left\langle \frac{dN(\vec{k}_{1\perp})}{d^2k_1 dy_1}[\rho_p, \rho_t] \frac{dN(\vec{k}_{2\perp})}{d^2k_2 dy_2}[\rho_p, \rho_t] \right\rangle \quad (16)$$

where brackets $\langle \cdot \rangle$ denote the statistical average over different realizations of the color charge configurations of the projectile and target, and

$$\frac{dN(\vec{k}_\perp)}{d^2kdy}[\rho_p, \rho_t] = \frac{dN^{\text{even}}(\vec{k}_\perp)}{d^2kdy}[\rho_p, \rho_t] + \frac{dN^{\text{odd}}(\vec{k}_\perp)}{d^2kdy}[\rho_p, \rho_t]. \quad (17)$$

We note that Eq. (16) relies on the fact that to leading order in α_s , the two-particle correlation function $\left. \frac{dN}{dy_1 d^2p_1 dy_2 d^2p_2} \right|_{\rho_p, \rho_t} = \left. \frac{dN}{dy_1 d^2p_1} \frac{dN}{dy_2 d^2p_2} \right|_{\rho_p, \rho_t}$ factorizes into a product of single particle distribution when evaluated for a fixed configuration of color charges of the projectile and target [7, 28–30]. Genuinely non-factorizable (“non-flow”) two-particle correlations e.g. due to di-jet production only appear at next-to-leading order in α_s ; however they have not been calculated in the dense-dense limit so far.

C. Dense-dense CYM

Notably the **dense-dense calculation** proceeds along very similar lines. Starting from the statistical sampling color charges in the projectile and target, one computes the light

like Wilson lines of both projectile and target in fundamental representation. Subsequently, the initial gauge fields in the forward light-cone (at $\tau = 0^+$) are determined according to the solution of the classical Yang-Mills equations, but now including the full non-linearity of projectile and target fields. Starting from these initial conditions, one then solves the classical Yang-Mills equations of motion in the forward light cone up to the time where observables are measured. Ultimately, one exploits the residual gauge freedom to fix Coulomb gauge at the time of the measurement and determines the spectrum of produced gluons $\frac{dN_g}{dyd\vec{p}_\perp}$ by projecting the gauge fields onto transversely polarized modes (c.f [31]). Details of the numerical procedure can be found in Ref. [7].

D. Numerical results

We now turn to the discussion of our numerical results and first study the overall multiplicity per unity rapidity $\left\langle \frac{dN_g}{dy} \right\rangle \equiv \int_{m/2} d^2\vec{p}_\perp \frac{dN_g}{dyd^2\vec{p}_\perp}$ and its variance $\left\langle \frac{dN_g}{dy} \frac{dN_g}{dy} \right\rangle - \left\langle \frac{dN_g}{dy} \right\rangle^2$ which are presented in Fig. 1. We first focus on the left panel, where we fix the saturation scale of the target $Q_s^{(A)} = 2.5$ GeV and investigate the dependence on the saturation scale $Q_s^{(P)}$ of the projectile, which as discussed in Sec. I, corresponds to the expansion parameter for the dilute-dense approximation. Since the multiplicity in dilute-dense calculations is directly proportional to $\left(Q_s^{(P)}\right)^2$ it is in fact sufficient to perform a single set of calculations shown as the single data point for $Q_s^{(P)} = 1$ GeV. Based on the analytical scaling $\langle dN/dy \rangle \propto \left(Q_s^{(P)}\right)^2$ of the dilute-dense formulae for the single inclusive production and $\left(Q_s^{(P)}\right)^4$ for the variance, one then obtains the result for all other values of $Q_s^{(P)}$ shown in terms of the solid lines. By comparing to the data-points of the full dense-dense (CYM) calculation, we find that such scaling is indeed well reproduced for $Q_s^{(P)} \lesssim 1$ GeV, where there is a good quantitative agreement between dilute-dense and dense-dense calculations.

However, for $Q_s^{(P)} \gtrsim 1$ GeV higher order saturation corrections become increasingly important and the dilute-dense approximation tends to over-predict particle production. While for single inclusive particle production higher order corrections remain on the order of $\sim 50\%$ even up to $Q_s^{(P)} \sim 4$ GeV, we find that double inclusive observables, such as the variance of the multiplicity, appear to be significantly more sensitive to higher-order saturation corrections. When considering $\left\langle \frac{dN_g}{dy} \frac{dN_g}{dy} \right\rangle - \left\langle \frac{dN_g}{dy} \right\rangle^2$, sizeable discrepancies on the order of $\sim 50\%$ between dilute-dense and dense-dense calculations already emerge for $Q_s^{(P)} \sim$

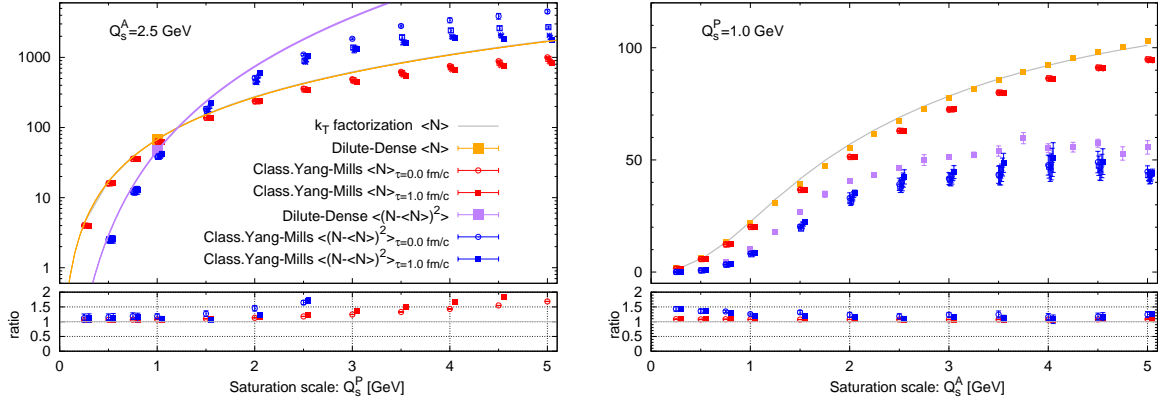


FIG. 1: Single inclusive multiplicity $\langle dN/dy \rangle$ and its variance (left) as a function of $Q_{s,0}^{(p)}$ and (right) as a function of $Q_{s,0}^{(A)}$. Different curves show results obtained from dilute-dense and dense-dense (Class. Yang-Mills) calculations. Gray line show an additional semi-analytic calculation based on k_t -factorization [8–10], which is equivalent to the leading order dilute-dense approximation for single inclusive production. Classical Yang-Mills results obtained for different times $\tau = 0.0, 0.2, 0.4, 0.6, 0.8, 1.0$ fm/c are shown as different symbols and have been offset horizontally for better visibility. Bottom panels show the ratio of dilute-dense to dense-dense at $\tau = 0$ (open circles) and $\tau = 1$ fm/c (full squares).

2 GeV and steadily increase for larger values of $Q_s^{(P)}$ where the dilute-dense approximation breaks down.

By fixing the saturation scale of the projectile $Q_s^{(P)}$ to a (small) value of 1 GeV we can further assess the $Q_s^{(A)}$ dependence of the dilute-dense approximation. We find that for such relatively small values of $Q_s^{(P)}$, the dilute-dense approximation provides a more or less uniform approximation of the dense-dense result, as is shown in the right panel of Fig. 1. Higher order saturation corrections to $\langle \frac{dN_g}{dy} \rangle$ and its variance are typically $\lesssim 20\%$ except perhaps for very small values of $Q_s^{(A)} \lesssim 1$ GeV, where the projectile effectively becomes more dense than the target. We also note that for the dense-dense calculation changes in the overall multiplicity as well as its fluctuations are relatively small over the course of the classical Yang-Mills evolution in the forward light-cone, indicating that the values inferred at $\tau = 0^+$ already provide a good estimate of the event-by-event gluon multiplicity.

Next we investigate the effects on azimuthal correlations between the produced gluons, which we will quantify in terms of Fourier coefficients $v_n\{2\}$ of the \vec{p}_\perp integrated two-particle

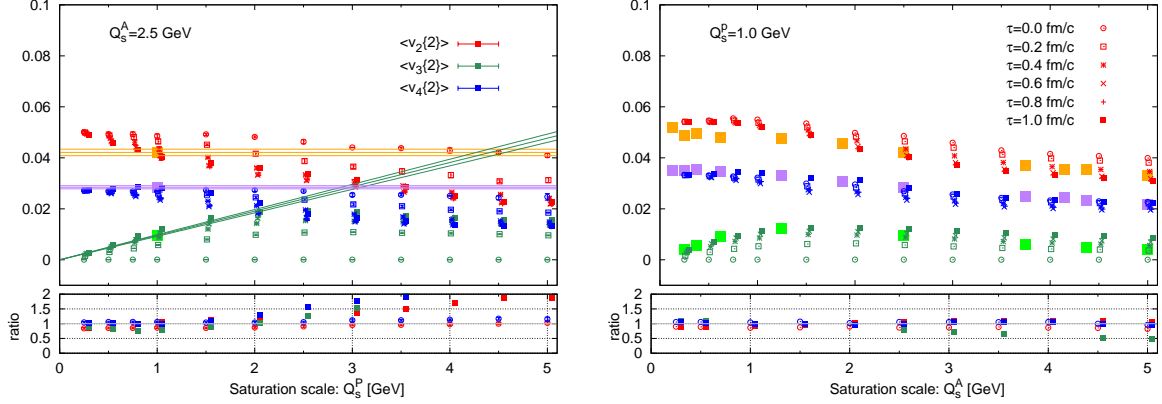


FIG. 2: Azimuthal anisotropy $v_n\{2\}$ (left) a function of $Q_{s,0}^{(p)}$ and (right) as a function of $Q_{s,0}^{(A)}$. Different curves show results obtained from dilute-dense and dense-dense (Class. Yang-Mills) calculations. Classical Yang-Mills results obtained for different times $\tau = 0.0, 0.2, 0.4, 0.6, 0.8, 1.0$ fm/c are shown as different symbols and have been offset horizontally for better visibility. Bottom panels show the ratio of dilute-dense to dense-dense at $\tau = 0$ (open circles) and $\tau = 1$ fm/c (full squares). Solid lines in the left panel are obtained using the scaling argument of Ref. [21] and represent $v_2, v_4 \propto (Q_s^{(P)})^0$ and $v_3 \propto Q_s^{(P)}$.

correlation function

$$v_n\{2\} = \sqrt{\frac{\langle b_n b_n^* \rangle}{\langle b_0 b_0^* \rangle}}, \quad b_n \equiv \int_{m/2} d^2 \vec{p}_\perp \frac{dN_g}{dy d^2 \vec{p}_\perp} e^{in\phi_{\vec{p}_\perp}}. \quad (18)$$

Such initial state azimuthal correlations reflect intrinsic correlations of gluons in the projectile and target [32, 33]; they are currently of particular phenomenological interest, as various studies have argued for their importance in understanding collective phenomena in small collision systems [19–22, 34], including p/d/He3+A collisions at RHIC as well as p+p and p+A collisions at the LHC.

We present a compact summary of our results for azimuthal correlations in Fig. 2, where we compare the results for v_2, v_3 and v_4 in dilute-dense and dense-dense calculations as a function of $Q_s^{(P)}$ and $Q_s^{(A)}$ in the left and right panels. While for small values of $Q_s^{(P)}$, the dense-dense calculation appears to be well approximated by the semi-analytic dilute-dense calculation, and shows the expected scaling of the different harmonics $v_2, v_4 \propto (Q_s^{(P)})^0$ and $v_3 \propto Q_s^{(P)}$ [21], the dilute-dense approximation starts to overpredict the azimuthal correlation strength for $Q_s^{(P)} \gtrsim 1$ GeV. We find that in this regime, the v_n 's obtained in the dense-dense calculation start to show a significant time dependence, clearly indicating the

importance of re-scattering in the forward light cone (in the “final state”), which are always associated with saturation corrections to the leading order dilute dense result. Specifically, the odd-harmonic v_3 increases from $v_3 = 0$ at $\tau = 0^+$ up to $v_3 \approx 2\%$ over the course of the classical Yang-Mills evolution, while the even harmonics v_2 and v_4 decrease by a comparable amount (see also [7]). Since for $Q_s^{(P)} \lesssim 2$ GeV the increase of v_3 is rather well described by the first saturation correction to dilute-dense limit (which gives zero v_3), it is conceivable that the observed decrease of the even harmonics could also be captured (at least partially) by the first saturation correction. Indeed, naive power counting argument in $Q_s^{(P)}$ predicts linear deviation of v_{even} from the dilute-dense regime. However, it is impossible to make this argument stronger, because, as discussed in Sec. I, the associated corrections to $d^2N_{\text{even}}/d^2k_1d^2k_2$ have not been calculated to date.

We also observe from the left panel of Fig. 2 that in order to obtain the phenomenologically relevant ordering of the different harmonics $v_2 > v_3 > v_4$, one needs to access relatively large values of $Q_s^{(P)}$ which appear to be outside the range of validity of the dilute-dense approximation (as demonstrated e.g. by v_3 deviating from its linear growth at lower $Q_s^{(P)}$). Vice versa for the relatively small values of $Q_s^{(P)} = 1$ GeV shown in the right panel, the even harmonics v_2 and v_4 exhibit a significantly smaller time dependence, resulting in $v_4 > v_3$ irrespective of the value of $Q_s^{(A)}$. We find that in this regime, where the dilute-dense approximation is justified, the $Q_s^{(A)}$ dependence of the dense-dense calculation is indeed well reproduced by the semi-analytic dilute-dense calculation, with typical errors on the 10% level for. This is, however, not the case for v_3 which is underpredicted by the dilute-dense approximation at large values of $Q_s^{(A)}$.

III. CONCLUSIONS

In this article, we presented for the first time a numerical study of higher order saturation corrections to the leading order dilute-dense approximation for different phenomenologically relevant observables. We explicitly demonstrated the expected deviations between the dilute-dense approximation and full dense-dense CYM simulations for single and double inclusive observables and showed that these deviation increase with the saturation momentum of the dilute projectile, as we anticipated based on the expansion (1). While for single inclusive observables, such as the average multiplicity $\langle dN_g/dy \rangle$, we find that the deviations remain

on the order of 50% even when the saturation scale of the projectile becomes on the same order as the saturation scale of the target ($Q_s^{(P)} \sim Q_s^{(A)}$), we find that double inclusive observables such as the azimuthal correlations v_n are significantly more sensitive to higher order saturation corrections.

When restricted to the range of validity, i.e. for $Q_s^{(P)} \ll Q_s^{(A)}$, we find that the dilute-dense approximation faithfully reproduces the dense-dense results, with almost uniform accuracy as a function of the saturation scale of the target $Q_s^{(A)}$. We find that in this regime, the dilute-dense approximation tends to over-predict particle production only by about 10(20)% compared to the corresponding dense-dense result for the single (double) inclusive gluon production.

Acknowledgements: We thank A. Dumitru, A. Kovner, Yu. Kovchegov, T. Lappi, M. Mace, L. McLerran, B. Schenke, P. Tribedy and R. Venugopalan for insightful discussions and collaboration on related projects. We gratefully acknowledge support by the Deutsche Forschungsgemeinschaft (DFG) through the grant CRC-TR 211 “Strong-interaction matter under extreme conditions” Project number 315477589 (S.S.) and by the US Department of Energy grant de-sc0020081 (V.S.). V.S. thanks the ExtreMe Matter Institute EMMI (GSI Helmholtzzentrum für Schwerionenforschung, Darmstadt, Germany) for partial support and hospitality.

-
- [1] Y. V. Kovchegov and E. Levin, *Quantum Chromodynamics at High Energy* (Cambridge University Press, 2012).
 - [2] Y. V. Kovchegov and V. V. Skokov, Phys. Rev. **D97**, 094021 (2018), 1802.08166.
 - [3] A. Krasnitz and R. Venugopalan, Phys. Rev. Lett. **84**, 4309 (2000), hep-ph/9909203.
 - [4] A. Krasnitz, Y. Nara, and R. Venugopalan, Nucl. Phys. **A727**, 427 (2003), hep-ph/0305112.
 - [5] T. Lappi, Phys. Rev. **C67**, 054903 (2003), hep-ph/0303076.
 - [6] J. P. Blaizot, T. Lappi, and Y. Mehtar-Tani, Nucl. Phys. **A846**, 63 (2010), 1005.0955.
 - [7] B. Schenke, S. Schlichting, and R. Venugopalan, Phys. Lett. **B747**, 76 (2015), 1502.01331.
 - [8] Y. V. Kovchegov and A. H. Mueller, Nucl. Phys. **B529**, 451 (1998), hep-ph/9802440.
 - [9] A. Dumitru and L. D. McLerran, Nucl. Phys. **A700**, 492 (2002), hep-ph/0105268.
 - [10] J. P. Blaizot, F. Gelis, and R. Venugopalan, Nucl. Phys. **A743**, 13 (2004), hep-ph/0402256.

- [11] A. Kovner and V. V. Skokov, Phys. Rev. **D98**, 014004 (2018), 1805.09296.
- [12] I. Balitsky, Phys. Rev. **D70**, 114030 (2004), hep-ph/0409314.
- [13] G. A. Chirilli, Y. V. Kovchegov, and D. E. Wertheim, JHEP **03**, 015 (2015), 1501.03106.
- [14] A. Kovner and M. Lublinsky, Int. J. Mod. Phys. **E22**, 1330001 (2013), 1211.1928.
- [15] Y. V. Kovchegov and D. E. Wertheim, Nucl. Phys. **A906**, 50 (2013), 1212.1195.
- [16] T. Altinoluk, N. Armesto, A. Kovner, and M. Lublinsky, Eur. Phys. J. **C78**, 702 (2018), 1805.07739.
- [17] A. Kovner and V. V. Skokov, Phys. Lett. **B785**, 372 (2018), 1805.09297.
- [18] L. McLerran and V. Skokov, Nucl. Phys. **A959**, 83 (2017), 1611.09870.
- [19] B. Schenke, S. Schlichting, P. Tribedy, and R. Venugopalan, Phys. Rev. Lett. **117**, 162301 (2016), 1607.02496.
- [20] M. Mace, V. V. Skokov, P. Tribedy, and R. Venugopalan, Phys. Rev. Lett. **121**, 052301 (2018), [Erratum: Phys. Rev. Lett.123,no.3,039901(2019)], 1805.09342.
- [21] M. Mace, V. V. Skokov, P. Tribedy, and R. Venugopalan, Phys. Lett. **B788**, 161 (2019), 1807.00825.
- [22] M. Mace, V. V. Skokov, P. Tribedy, and R. Venugopalan (2019), 1901.10506.
- [23] S. Schlichting and B. Schenke, Phys. Lett. **B739**, 313 (2014), 1407.8458.
- [24] H. Mäntysaari, B. Schenke, C. Shen, and P. Tribedy, Phys. Lett. **B772**, 681 (2017), 1705.03177.
- [25] L. McLerran and P. Tribedy, Nucl. Phys. **A945**, 216 (2016), 1508.03292.
- [26] B. Schenke, P. Tribedy, and R. Venugopalan, Phys. Rev. Lett. **108**, 252301 (2012), 1202.6646.
- [27] B. Schenke, P. Tribedy, and R. Venugopalan, Phys. Rev. **C86**, 034908 (2012), 1206.6805.
- [28] F. Gelis, T. Lappi, and R. Venugopalan, Phys. Rev. **D78**, 054020 (2008), 0807.1306.
- [29] F. Gelis, T. Lappi, and R. Venugopalan, Phys. Rev. **D79**, 094017 (2009), 0810.4829.
- [30] T. Lappi, S. Srednyak, and R. Venugopalan, JHEP **01**, 066 (2010), 0911.2068.
- [31] J. Berges, K. Boguslavski, S. Schlichting, and R. Venugopalan, Phys. Rev. **D89**, 114007 (2014), 1311.3005.
- [32] T. Lappi, B. Schenke, S. Schlichting, and R. Venugopalan, JHEP **01**, 061 (2016), 1509.03499.
- [33] T. Altinoluk, N. Armesto, G. Beuf, A. Kovner, and M. Lublinsky, Phys. Lett. **B751**, 448 (2015), 1503.07126.
- [34] M. Greif, C. Greiner, B. Schenke, S. Schlichting, and Z. Xu, Phys. Rev. **D96**, 091504 (2017),

1708.02076.